PHYSICAL REVIEW A **95**, 012705 (2017)

Relative dissociation fractions of N_2O under 15–30-keV H^-, C^-, and O^- negative-ion impact

Dedong Wang, Guannan Guo, Guangxin Min, and Xuemei Zhang[*]
Institute of Modern Physics, Fudan University, Shanghai 200433, China and Applied Ion Beam Physics Laboratory, Fudan University, Key Laboratory of the Ministry of Education, China

(Received 19 November 2016; published 20 January 2017)

The relative dissociation fractions of N_2O are studied under 15–30-keV negative ions H^-,C^-, and O^- impact. The recoil ions and ion pairs originating from the target molecule N_2O are detected and identified in coincidence with scattered ions in single electron loss (SL) and double electron loss (DL) channels using a time-of-flight mass spectrometer. The dissociation fractions for the production of the fragment ions are obtained. We find that the relative dissociation fractions in SL are smaller than those in DL, and the degree of fragmentation will become greater with the impact energy increasing. We also analyze the coincident TOF spectra of two fragment ions which are produced from dissociation of N_2O^{2+} and give the possible dissociation pathways of N_2O^{2+} with 15–30-keV H^-,C^-, and O^- impact. There are many studies on N_2O with positive-ion, photon, and electron impact, and we compare our results under negative-ion impact with those works.

DOI: 10.1103/PhysRevA.95.012705

I. INTRODUCTION

The nitrous oxide molecule, as known as laughing gas, is an important greenhouse gas. It is a trace gas representing a very small fraction of the total atmospheric gases, but has about 300 times more warming potential as a greenhouse gas than carbon dioxide, CO_2 [1]. Nitrous oxide also causes ozone depletion. A new study suggests that N_2O emission currently is the single most important ozone-depleting substance and is expected to remain the largest throughout the 21st century [2,3]. Therefore, the N_2O molecule has gained the attention of many experimental [4,5], theoretical [6], and computational physicists. The ionization and dissociation studies are mostly focused on positive ions, photons, and electron impact [7–18]. So far, there is no study on the relative dissociation fractions of N_2O for negative-ion impact.

When the negative ion collides with target gases, the projectile may lose no electrons, one electron, or two electrons. The process when negative ions lose one electron is called a single-electron-loss (SL) channel, and the process when negative ions lose two electrons is called a double-electron-loss (DL) channel. We do not study the process in which the projectile loses no electrons.

During N_2O colliding with a negative ion, the target N_2O could be excited, ionized to a single-, double-, or multiple-charge state. Many fragments could be produced from the excited N_2O molecule or ionization dissociation. In our study, we observe singly charged fragment ions, and we also find ion pairs due to the production of N_2O^{2+}.

In the present work, the relative dissociation fractions for the production of the fragment ions of N_2O are studied under 15–30-keV H^-, C^-, and O^- impact. By using a time-of-flight mass spectrometer (TOFMS), we detect and identify the recoil ions and ion pairs produced from the target molecule N_2O in coincidence with scattered ions in SL and DL channels.

II. APPARATUS AND EXPERIMENTAL METHOD

The apparatus has been used in our previous works [19–22]; the details are described in [19]. Now, we only give a schematically brief description. Figure 1 shows the apparatus which consists of a negative-ion source, analyzing magnet, switching magnet, a TOFMS with an anode plate detector, a position-sensitive delay-line detector, two deflectors, and a Faraday cup. The negative ions are produced and extracted from a cesium-sputtered negative-ion source (CSNIS), and according to their mass-to-charge ratio, they are analyzed and chosen by a 90° bending magnet, and then the chosen negative ions are focused and collimated before entering the collision chamber. In the chamber, the incident negative ions are made to cross a gas beam at right angles which effuses from a grounded hypodermic needle, and the detection system is mutually perpendicular to them. The electric-field direction of TOFMS is orthogonal with the gas jet target. After the negative ions collide with the gas target, most negative ions do not lose any electrons and are not detected but are collected by a Faraday cup (FC). The produced neutrals when negative ions lose one electron or positive ions when negative ions lose two electrons are detected by the position sensitive delay-line detector. The recoil ions which are produced from the target gas are accelerated by a homogeneous electric field (75–120 V/cm) and pass through the field-free drift tube, and finally are detected by the anode plate detector. The gas flow of N_2O with a specified purity of 99.99% is controlled by a fine needle valve. We use a turbo molecular pump backed by a rotary pump to maintain the base pressure of the chamber at about 7.5×10^{-8} Torr. The typical working pressure is about 1×10^{-6} Torr with gas load.

The data acquisition system has been described in our previous works [20]. We use a multihit time-to-digital converter

---

[*] zhangxm@fudan.edu.cn

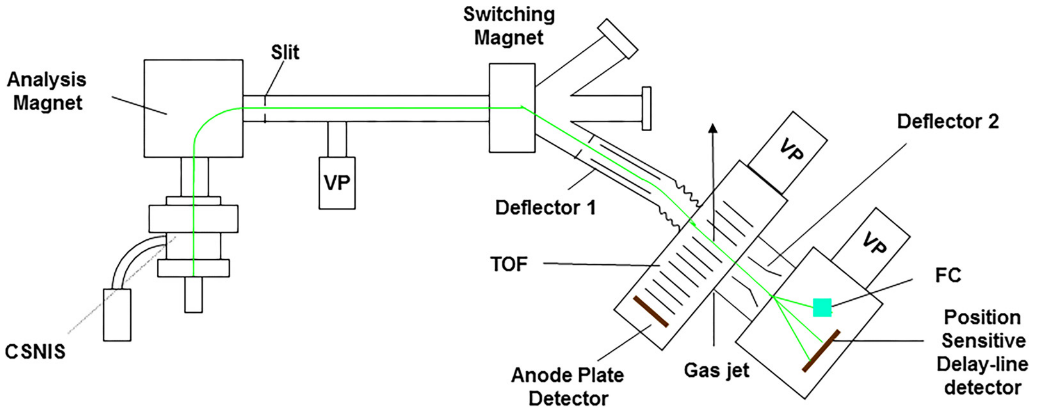

FIG. 1. Schematic diagram of the experimental setup. CSNIS, VP, TOFMS, and FC represent Cs-sputtered negative-ion source, vacuum pump, time-of-flight mass spectrometer, and Faraday cup.

(TDC) to measure two or more fragment ions produced in a single collision.

In our work, the relative dissociation fraction $f(X)$ to produce recoil ion X is defined by

$$f(X)=\frac{\frac{N(X)}{\varepsilon(X)\mu(X)}}{\frac{N(\mathrm{N_2O^+})}{\varepsilon(\mathrm{N_2O^+})\mu(\mathrm{N_2O^+})}+\frac{N(\mathrm{O^+})}{\varepsilon(\mathrm{O^+})\mu(\mathrm{O^+})}+\frac{N(\mathrm{N^+})}{\varepsilon(\mathrm{N^+})\mu(\mathrm{N^+})}+\frac{N(\mathrm{NO^+})}{\varepsilon(\mathrm{NO^+})\mu(\mathrm{NO^+})}+\frac{N(\mathrm{N_2}^+)}{\varepsilon(\mathrm{N_2}^+)\mu(\mathrm{N_2}^+)}},$$

where $N(X)$ is the collected number of X ions produced in the collision between negative ions and N_2O, and X can be N^+, O^+, $N_2{}^+$,NO^+. ε is the detection efficiency of the recoil ion detector, μ is the collection efficiency of the TOFMS.

In this work, the energy of recoil ions with $q = 1$ and $q = 2$ when hitting on the detector is about 4 and 8 keV. So we assume $\varepsilon(X)$ is almost the same for different recoil ions within an error of about 5%. In order to ensure that all recoil ions can be collected, we apply the voltages on the TOFMS at 75–120 V/cm in the present experiments. Thus, for different recoil ions, we consider that $\mu(X)$ is nearly the same within an error of about 4.4%. The description about the ε and μ in detail can be found in our previous works [19,20,21]. Including the above premises, the relative dissociation fraction $f(X)$ can be expressed by

$$f(X)=\frac{N(X)}{N(\mathrm{N_2O^+})+N(\mathrm{O^+})+N(\mathrm{N^+})+N(\mathrm{NO^+})+N(\mathrm{N_2}^+)}.$$

III. RESULTS AND DISCUSSION

Figure 2 shows typical TOF spectra of recoil ions under 30-keV H^-, C^-, O^- impact in SL and DL processes. Due to rather low time resolution, we could not distinguish N^+ and O^+, NO^+ and $N_2{}^+$ effectively. So we use Lorentz line shape fitting to distinguish them, and the red and green lines in Fig. 2 are the fitting lines.

We obtain the relative dissociation fractions for the production of N^+, O^+, $N_2{}^+$, NO^+ through analyzing these TOF spectra. The relative dissociation fractions for the production of N^+, O^+, $N_2{}^+$, NO^+ are presented in Table I. The total uncertainties of the results for N^+, O^+, $N_2{}^+$, NO^+ are about 7.3%, and they mainly consist of four parts: the uncertainty of detection efficiency (5%), the collection efficiency error of TOFMS (4.4%), the statistical error (0.7%), and the Lorentz fitting error (3%). The fractions are also plotted in Fig. 3 in order to see more clearly. From Fig. 3 and Table I, we can find the following four points. First, with the impact energy increasing, the relative numbers of produced atomic ions become bigger and bigger, and the fractions of molecular ions become smaller. That means the target molecules fragment more often with bigger incident energy. As we know, N_2O is a linear asymmetric molecule; its ground state is $X\ {}^1\Sigma^+$ with electronic configuration $(1\sigma)^2(2\sigma)^2(3\sigma)^2(4\sigma)^2(5\sigma)^2(6\sigma)^2(1\pi)^4(7\sigma)^2(2\pi)^4$. When one outmost 2π electron is removed, the ground state of N_2O^+ $X\ {}^4\Pi$ is formed. If one inner shell electron is removed, an excited molecular ion state will be produced. When one 7σ electron is removed, the first excited state is $A\ {}^2\Sigma^+$. If one 1π electron is removed, $B\ {}^4\Pi$ is produced. If one 6σ electron is removed, $C\ {}^2\Sigma^+$ is formed. Itis found [23] that the major production of N_2O^+ with single-hole out valence states (including $A\ {}^2\Sigma^+, B\ {}^4\Pi$, and $C\ {}^2\Sigma^+$) is NO^+, whereas with inner valence states is $N_2{}^+$. The first excited state $A\ {}^2\Sigma^+$ could only fast dissociate (dissociate before rotation) into $NO^+ + N$; the higher $B\ {}^2\Pi$ and $C\ {}^2\Sigma^+$ states could fast dissociate into not only $NO^+ + N$, but $N_2{}^+ + O$.N^+, O^+ were also found when dissociation happened with the $C\ {}^2\Sigma^+$ state, although O^+ is produced to a small extent. In Fig. 3, the appearance of N^+, O^+ means at least the $C\ {}^2\Sigma^+$ state is already produced with 15–30-keV H^-, C^-, O^- impact. With impact energy increasing, more and more N^+, O^+ produced means the number of N_2O^+ excited to at least the $C\ {}^2\Sigma^+$ state increases, too. Second, the fractions of N^+, O^+ in the DL process are larger than those in the SL process for certain impact energies and certain incident ions. From Fig. 2, it can also be seen that fewer N_2O^+ are left in the DL spectra, especially with C^- and O^- impact. In our previous work [21,22], we have mentioned

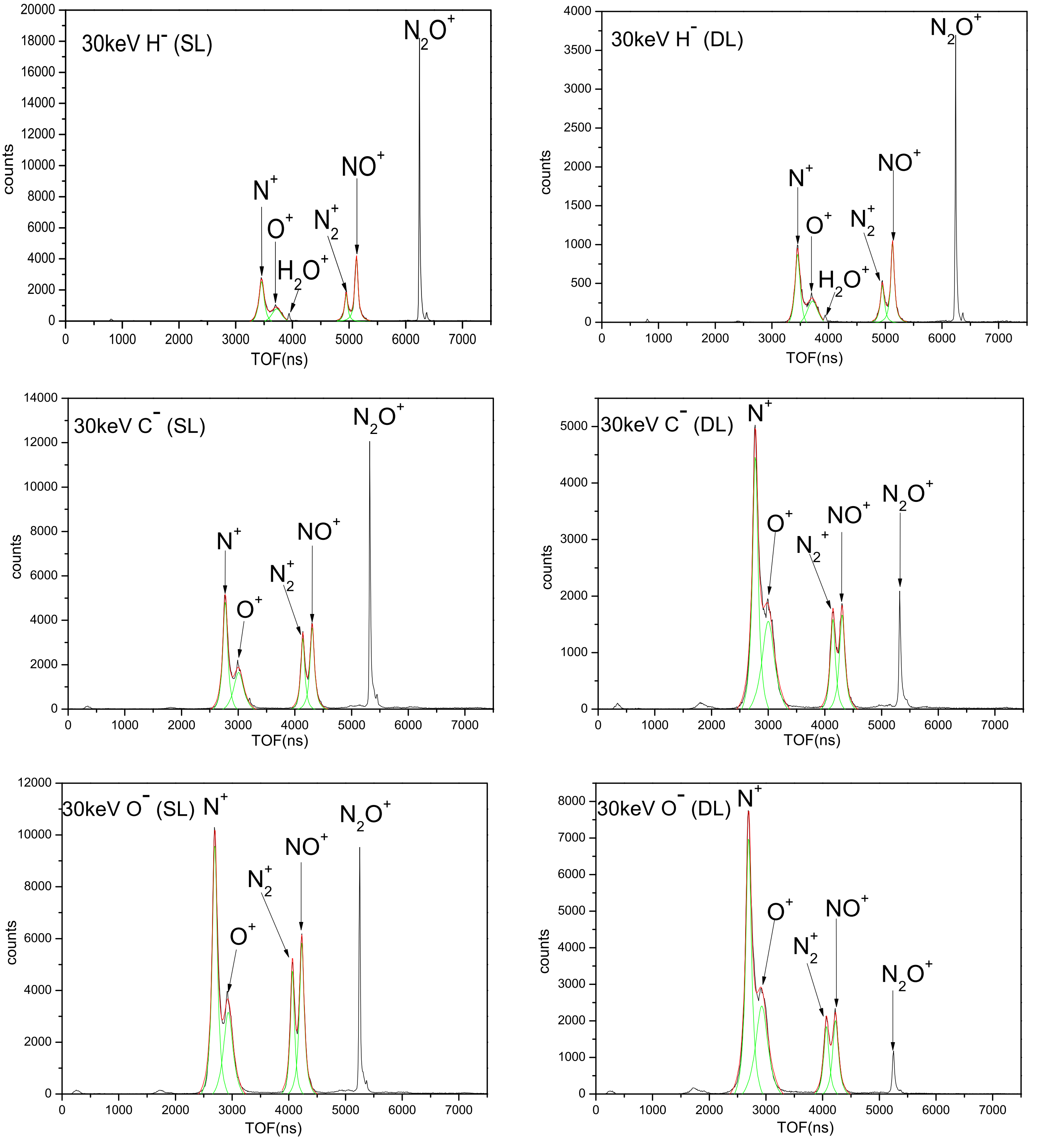

FIG. 2. TOF spectra of recoil ions in SL and DL processes formed by 30-keV H^-, C^-, and O^- impact on N_2O.

that small impact parameter collisions occur preferentially in the DL process. It is also pointed out that the transferred energy from the projectile to the targets is larger at the smaller impact parameter and the energy is transferred mainly to the inner shell electrons. In the DL process, inner shell electrons in the target have a bigger opportunity to be removed than in the SL process. The produced excited N_2O^+ states are unstable; fast dissociation causes fewer N_2O^+ left. N^+ and O^+ could be produced when N_2O^+ is excited to high enough states. Thus, there are larger fractions of atomic ions in the DL process than in SL. Third, comparing the results of H^- with that of C^- and O^-, it is found that the fragment ion with the least fraction is different. With H^- impact, $N_2{}^+$ is the least. However, with C^- or O^- impact, N_2O^+ is the one. It means the precursor ion has bigger probabilities to fragment with C^- or O^- incident. Since the impact energy regions of H^-,C^-, and O^- are the

TABLE I. The relative dissociation fractions of N_2O under 15–30-keV H^-, C^-, and O^- impact.

			H^- (SL)		
	N^+	O^+	N_2^+	NO^+	N_2O^+
30 (keV)	0.235 ± 0.017	0.209 ± 0.015	0.092 ± 0.007	0.224 ± 0.016	0.241 ± 0.018
25 (keV)	0.229 ± 0.017	0.221 ± 0.016	0.092 ± 0.007	0.223 ± 0.016	0.235 ± 0.017
20 (keV)	0.231 ± 0.017	0.209 ± 0.015	0.096 ± 0.007	0.230 ± 0.017	0.234 ± 0.017
15 (keV)	0.202 ± 0.015	0.189 ± 0.014	0.100 ± 0.007	0.252 ± 0.018	0.256 ± 0.019
			H^-(DL)		
	N^+	O^+	N_2^+	NO^+	N_2O^+
30 (keV)	0.258 ± 0.019	0.261 ± 0.019	0.107 ± 0.008	0.199 ± 0.015	0.175 ± 0.013
25 (keV)	0.264 ± 0.019	0.234 ± 0.017	0.113 ± 0.008	0.201 ± 0.015	0.188 ± 0.014
20 (keV)	0.261 ± 0.019	0.236 ± 0.017	0.114 ± 0.008	0.200 ± 0.015	0.189 ± 0.014
15 (keV)	0.240 ± 0.017	0.209 ± 0.015	0.124 ± 0.009	0.218 ± 0.016	0.210 ± 0.015
			C^- (SL)		
	N^+	O^+	N_2^+	NO^+	N_2O^+
30 (keV)	0.266 ± 0.019	0.230 ± 0.017	0.152 ± 0.011	0.195 ± 0.014	0.157 ± 0.011
25 (keV)	0.262 ± 0.019	0.227 ± 0.017	0.152 ± 0.011	0.203 ± 0.015	0.156 ± 0.011
20 (keV)	0.263 ± 0.019	0.190 ± 0.014	0.166 ± 0.012	0.220 ± 0.016	0.161 ± 0.012
15 (keV)	0.242 ± 0.018	0.166 ± 0.012	0.164 ± 0.012	0.254 ± 0.019	0.174 ± 0.013
			C^- (DL)		
	N^+	O^+	N_2^+	NO^+	N_2O^+
30 (keV)	0.350 ± 0.026	0.337 ± 0.025	0.122 ± 0.009	0.139 ± 0.010	0.051 ± 0.003
25 (keV)	0.320 ± 0.024	0.352 ± 0.026	0.124 ± 0.009	0.149 ± 0.011	0.054 ± 0.004
20 (keV)	0.318 ± 0.023	0.310 ± 0.023	0.147 ± 0.011	0.168 ± 0.012	0.057 ± 0.004
15 (keV)	0.309 ± 0.022	0.277 ± 0.020	0.150 ± 0.011	0.198 ± 0.014	0.066 ± 0.006
			O^- (SL)		
	N^+	O^+	N_2^+	NO^+	N_2O^+
30 (keV)	0.338 ± 0.025	0.246 ± 0.018	0.142 ± 0.010	0.197 ± 0.014	0.078 ± 0.006
25 (keV)	0.323 ± 0.024	0.243 ± 0.018	0.142 ± 0.010	0.210 ± 0.015	0.083 ± 0.006
20 (keV)	0.310 ± 0.023	0.222 ± 0.016	0.144 ± 0.011	0.225 ± 0.016	0.099 ± 0.007
15 (keV)	0.271 ± 0.020	0.199 ± 0.015	0.153 ± 0.011	0.267 ± 0.019	0.110 ± 0.008
			O^- (DL)		
	N^+	O^+	N_2^+	NO^+	N_2O^+
30 (keV)	0.389 ± 0.028	0.360 ± 0.026	0.105 ± 0.008	0.123 ± 0.009	0.023 ± 0.002
25 (keV)	0.377 ± 0.027	0.343 ± 0.025	0.111 ± 0.008	0.141 ± 0.010	0.027 ± 0.002
20 (keV)	0.349 ± 0.025	0.318 ± 0.023	0.126 ± 0.009	0.171 ± 0.012	0.036 ± 0.003
15 (keV)	0.312 ± 0.023	0.299 ± 0.022	0.143 ± 0.010	0.200 ± 0.015	0.046 ± 0.003

same, the most important factor to influence the dissociation seems to be not the impact energy but the impact momentum. So we analyze the data according to the impact momentum in the following paragraph. Fourth, the relative amounts of N_2^+ in SL and DL processes are different with H^- impact from those with C^- and O^- impact. For H^-, the fractions in SL are smaller than those in DL. But for C^- and O^-, the fractions are almost the same in the two processes. Due to more N_2^+ and O^+ produced in DL, it seems the N-O bonding is easier to be broken in DL than in SL with H^- impact. The extra O^+ comes from the N-O bonding being broken. However, with C^- and O^- impact, the fractions of N_2^+ remain almost unchanged. We propose that the extra O^+ may come from the direct dissociation $N_2O^+ \rightarrow N + O^+ + N$ or the following two step dissociation: $N_2O^+ \rightarrow NO^+ + N, NO^+ \rightarrow N + O^+$. We can see from the data of O^- that the decrease of N_2O^+ (about 6%) is smaller than the increase of O^+ (about 10%). So there must be some O^+ coming from NO^+. It means NO^+, which is a fragmental part of the direct dissociation of N_2O^+, is still populated in its highly excited state and could dissociate further.

In Fig. 4, we give the TOF spectrum of the produced ions following direct and dissociative ionization of a N_2O molecule by impact of 10-keV electrons [18]. We find the N_2O^+ peak is much higher than the others, which is similar to our results in H^- impact. But the ratio N_2^+/NO^+ is different from our results in H^- impact—it is much smaller. Compared with more results with electron impact [15–18], we find that the results under electron impact are similar to our results in H^- impact, but different from the results in C^- and O^- impact. The fraction of N_2O^+ is bigger than ours, and the fractions of N_2^+, O^+, N^+ are smaller. It means N_2O^+ populate rather lowly excited states and are more difficult to dissociate to other fragments. Meanwhile, the fractions of NO^+ are usually bigger in those works than ours, and the reason, as we mentioned, may be that NO^+ in our work still populates its highly excited state and could dissociate further.

In order to compare with our previous works, we give the curves of the relative fractions to N_2O^+ for production of N^+, O^+, N_2^+, NO^+ as a function of the momentum under 15–30-keV negative ions impact in SL and DL processes in Fig. 5. It seems that the fractions become greater with the

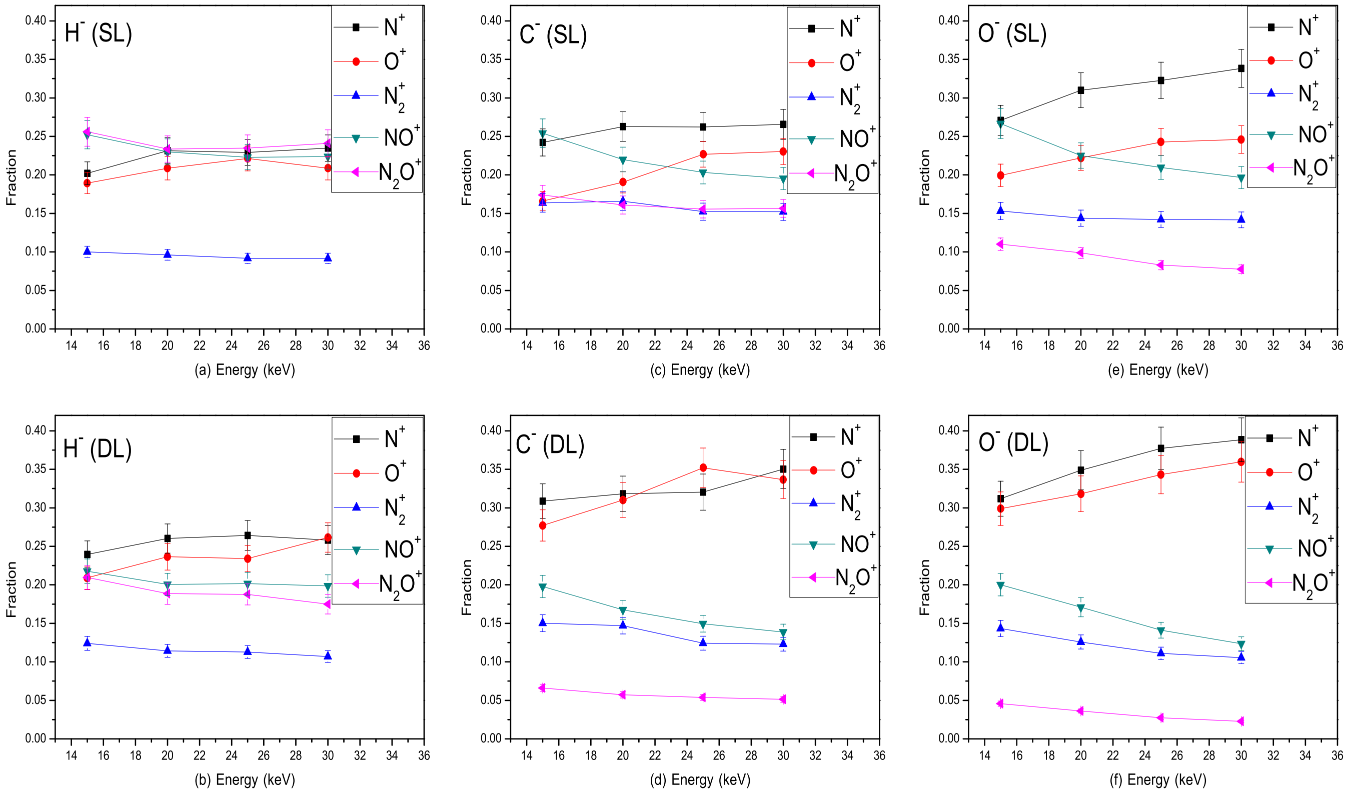

FIG. 3. The relative dissociation fractions of N_2O by H^-,C^-, and O^- impact in 1–30-keV energy region.

projectile momentum increasing, especially for smaller mass fragments N^+ and O^+. The fractions increase more quickly in DL processes than those in SL processes. We can find a similar phenomenon in our previous work for CO_2,CF_4, and SF_6 [20–22].

There are some ion pairs produced in the collision. The ion pairs include $N^+ + NO^+$, $O^+ + N_2{}^+$, $O^+ + N^+$, $N^+ + N^+$, etc. Figure 6 shows a coincidence spectrum of N_2O under the 30 keV O^- impact for a process as an example in order to study the dissociation channel. The coincidence spectra are given by using the same methods of Lange *et al.*'s work [24]. In Fig. 6, there are mainly four coincidence islands: $N^+ + NO^+$, $O^+ + N_2{}^+$, $O^+ + N^+$, and $N^+ + N^+$. The peak slope of N^+ and NO^+ is about -1, which suggests a direct breakup process: $N_2O^{2+} \rightarrow N^+ + NO^+$; the slope of O^+ and $N_2{}^+$ is about -1, which also indicates a direct breakup process: $N_2O^{2+} \rightarrow O^+ + N_2{}^+$; the slope of O^+ and N^+ is less than -1, and is indicative of two possible processes. One

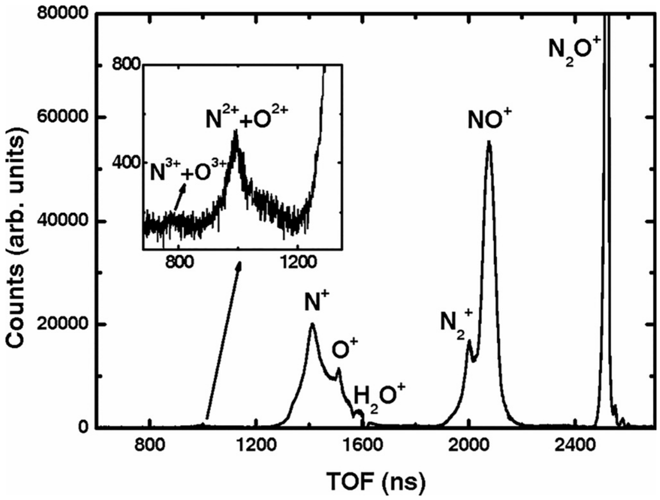

FIG. 4. TOF spectrum (background subtracted) of the produced ions following direct and dissociative ionization of a N_2O molecule by impact of 10-keV electrons [18].

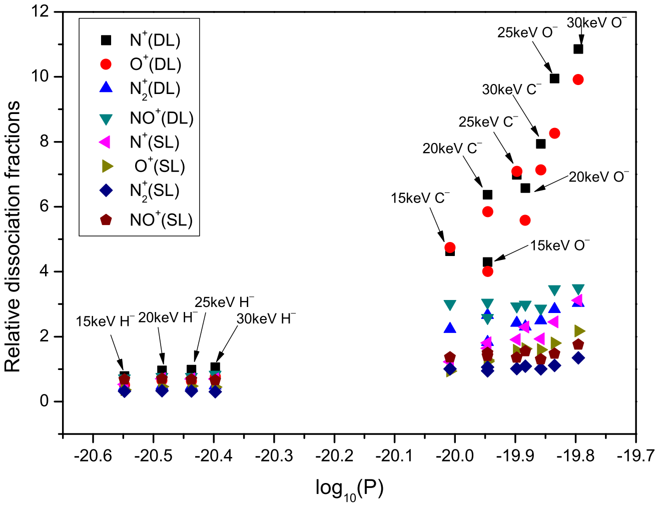

FIG. 5. The relative dissociation fractions of N_2O^+ as a function of the momentum of impacting negative ions. The momentum P is in kg m/s.

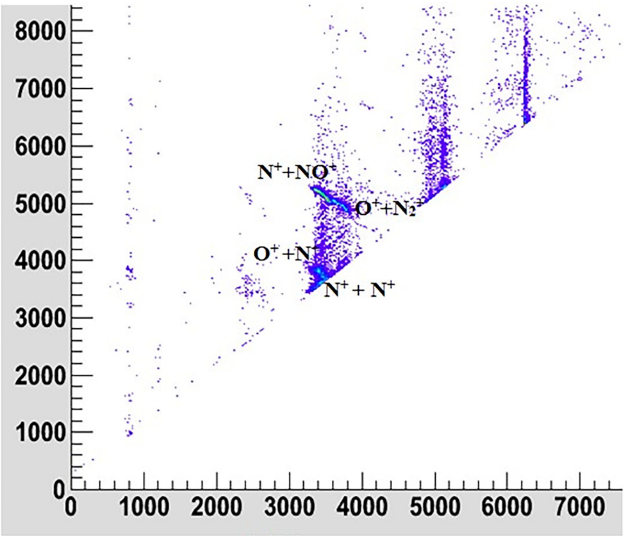

FIG. 6. A coincidence spectrum (vertical axis is flight time of the second fragment ion and horizontal axis is flight time of the first fragment ion) under 30-keV O^- impact for the SL channel.

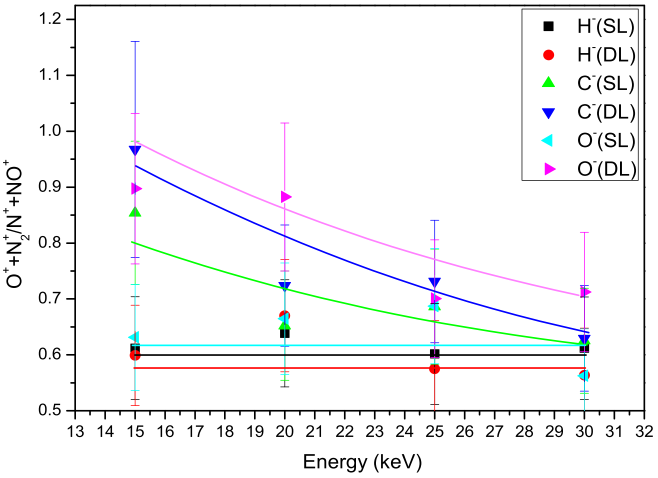

FIG. 7. The ratios of $O^+ + N_2{}^+/N^+ + NO^+$ under H^-,C^-, and O^- impact in 15–30-keV energy region. The curves are the eye-guide lines.

is $N_2O^{2+} \rightarrow N + NO^{2+}$,$NO^{2+} \rightarrow O^+ + N^+$, and the other is $N_2O^{2+} \rightarrow N^+ + NO^+$, $NO^+ \rightarrow N + O^+$. Besides, we can also observe the ion pairs of N^+ and N^+ in the coincidence spectrum. However, the slope might be affected by the electric noise along the diagonal line, and we could not give the peak slope of it. Thus, no process to produce N^+ and N^+ is given in this work.

We can obtain the ratio $O^+ + N_2{}^+/N^+ + NO^+$ from the coincidence spectrum in Fig. 6. Table II and Fig. 7 show the curves of the ratios of $O^+ + N_2{}^+/N^+ + NO^+$ under 15–30-keV H^-, C^-, and O^- impact. There is a declining trend for the ratio with energy increasing, especially under C^- and O^- impact. Because of the few counts and unsharp boundary, the uncertainties of the results are up to about 15%. Table II shows the relative dissociation fractions (%) for two coincidence channels with the earlier reported experimental results and a theoretical model. The ion pairs $(O^+, N_2{}^+)(N^+,NO^+)$ are produced by double ionization of N_2O. Due to its short lifetime (10 ns), no N_2O^{2+} is found in the TOF spectra. When two 2π electrons are removed from N_2O, the ground state of N_2O^{2+} $^3\Sigma^-$, the first excited state $^1\Delta$ could be produced. The $^3\Sigma^-$ state dissociates into $NO^+ + N^+$ or $N_2{}^+ + O^+$ by 3:1. The $^1\Delta$ state could only dissociated into $NO^+ + N^+$. The lower excited state of N_2O^{2+}, such as $^1\Sigma^+[1\pi^{-1},2\pi^{-1}]$ and $^1\Pi[7\sigma^{-1},1\pi^{-1}]$, could dissociate to $NO^+ + N^+$ or $N_2{}^+ + O^+$. When one or two innermost σ electrons are removed, N-O bonding could be broken with N-N bonding being broken simultaneously. A new dissociation channel $N^+ + O^+ + N$ is opened [5]. From Tables II and III, the bigger ratio of $O^+ + N_2{}^+/N^+ + NO^+$ means a bigger probability to break N-O bonding with ions' impact than with photon or electron impact. The smaller ratio with 24–100-nm photons may be caused by the first excited-state $^1\Delta$ population. Comparing the ratios of our work with that of Xe^{43+}, the ratios with H^- are almost the same as those with Xe^{43+}, however the values for C^- or O^- are bigger, especially in DL processes. Maybe in the low velocity region, the collision time is one important parameter to influence the dissociation of the double charged ions.

TABLE II. The ratios of $O^+ + N_2{}^+/N^+ + NO^+$ under 15–30-keV H^-, C^-, and O^- impact.

	$O^+ + N_2{}^+/N^+ + NO^+$					
	H^- (SL)	H^- (DL)	C^- (SL)	C^- (DL)	O^- (SL)	O^- (DL)
30 (keV)	0.61	0.56	0.63	0.63	0.56	0.71
25 (keV)	0.60	0.58	0.69	0.73	0.69	0.70
20 (keV)	0.64	0.67	0.65	0.72	0.66	0.88
15 (keV)	0.61	0.60	0.85	0.97	0.63	0.90

In the TOF spectra, we find that the widths of fragment ion NO^+ and $N_2{}^+$ are significantly bigger than that of the parent ion N_2O^+. The reason is the bigger translational energy of fragment ions obtained from the dissociation. The fragment ions with initial velocity towards the detector arrive earlier than those with initial velocity away from the detector. The peak width consists of two parts: the apparatus resolution and recoil velocity distribution. Thus, we assume the peak width of the parent ion N_2O^+ is entirely from the apparatus resolution. And then we obtain the recoil velocity width by removing the peak width of the parent ion N_2O^+ from the widths of NO^+ and $N_2{}^+$ using deconvolution. Eventually, the total translational energy of $(N + NO^+)$ and $(O + N_2{}^+)$ can be given by following formula [27]:

$$E_{t1} = \frac{m_{N_2O^+}}{4m_{NO^+}m_N}\left(\frac{eV}{d}\right)^2\Delta t^2,$$

$$E_{t2} = \frac{m_{N_2O^+}}{4m_O m_{N_2^+}}\left(\frac{eV}{d}\right)^2\Delta t^2,$$

where $m_{N_2O^+}$, m_{NO^+}, $m_{N_2^+}$, m_N, m_O are the parent ion N_2O^+ mass, fragment ion NO^+, and $N_2{}^+$ mass, fragment N and O mass; e is the elementary charge; V is the extraction voltage;

TABLE III. Comparison of the relative fractions of two coincidence channels with the earlier reported experimental results and a theoretical model [6].

Coincidence channel	10-keV electron [4]	24–100-nm photons [5]	800-nm intense laser [25]	40-eV photons [1]	5.9 MeV/u Xe^{43+} ions [26]	Theoretical prediction [6]
$O^+ + N_2{}^+$	21.20%	20.80%	24.20%	25%	41%	25%
$N^+ + NO^+$	60.20%	77.90%	74.40%	75%	59%	75%
$O^+ + N_2{}^+/N^+ + NO^+$	0.352	0.267	0.325	0.333	0.695	0.333

d is the distance between two plates in the ionization region; Δt is the recoil velocity width of recoil ion.

From Fig. 6, we can obtain the numbers of $N^+ + NO^+$ and $O^+ + N_2{}^+$, and this can represent the yield of doubly charged ions. Although there are doubly charged ions produced, the yield of doubly charged ions is only about 4% compared to that of singly charged ions. So we assume NO^+ and $N_2{}^+$ are only from the dissociation of N_2O^+. And the pathway of NO^+ is $N_2O^+ \rightarrow N + NO^+$; the pathway of $N_2{}^+$ is $N_2O^+ \rightarrow O + N_2{}^+$. In this premise, we can use the formulas E_{t1} and E_{t2} to calculate the total translational energy of the fragment ions.

Table IV shows the total translational energies of the fragments ($N + NO^+$) and ($O + N_2{}^+$). Figure 8 shows an adiabatic correlation diagram for N_2O^+ following Richard-Viard [23]. From Table III and Fig. 8, we can observe the following four points. First, the results under C^- and O^- impact are usually bigger than that under H^- impact. According to the law of conservation of energy, the transferred energy from the negative ion to N_2O is the sum of the translational energy of fragments, internal energy of the fragments, and the dissociation energy. The transferred energies are much bigger under C^- and O^- impact than that under H^- impact, so the parent ion N_2O^+ under C^- and O^- impact must populate on higher excited states. From Fig. 8 we can see that N_2O^+ may mainly populate a $A\ {}^2\Sigma^+$ or $B\ {}^2\Pi$ excited state for H^- impact, and the main dissociation pathways for $N_2O^+(A\ {}^2\Sigma^+, B\ {}^2\Pi)$ are $N_2O^+(A\ {}^2\Sigma^+, B\ {}^2\Pi) \rightarrow NO^+(X\ {}^1\Sigma^+) + N({}^2P)$ and $N_2O^+(A\ {}^2\Sigma^+, B\ {}^2\Pi) \rightarrow NO^+(X\ {}^1\Sigma^+) + N({}^2D)$ [28,29]. However, N_2O^+ may mainly populate the highly excited state $C\ {}^2\Sigma^+$ or $1\ {}^4\Sigma^-$ for C^- and O^- impact, and the main dissociation pathways for $N_2O^+(C\ {}^2\Sigma^+, 1\ {}^4\Sigma^-)$ are $N_2O^+(C\ {}^2\Sigma^+, 1\ {}^4\Sigma^-) \rightarrow NO^+(X\ {}^1\Sigma^+) + N({}^4S)$. So the fragment ions produced from higher excited states N_2O^+ have more translational energy. Second, the total translational energies in the DL process are larger than those in the SL process for certain energies. As we mentioned above, the DL process is preferred for small impact parameter collisions, and the transferred energy from the projectile to the target is larger at the smaller impact parameter. So the fragments have more energy in DL processes. Third, the translational energies of ($N + NO^+$) are usually larger than those of ($O + N_2{}^+$) except in H^- (DL) process. For H^- impact, the parent ion N_2O^+ populates its lowly excited state due to little transferred energy. For H^- impact in a SL process, as we mentioned, the main dissociation pathways for N_2O^+ are $N_2O^+(A\ {}^2\Sigma^+, B\ {}^2\Pi) \rightarrow NO^+(X\ {}^1\Sigma^+) + N\,({}^2\Pi), N_2O^+(A\ {}^2\Sigma^+, B\ {}^2\Pi) \rightarrow NO^+(X\ {}^1\Sigma^+) + N({}^2D)$, and $N_2O^+(A\ {}^2\Sigma^+, B\ {}^2\Pi) \rightarrow N_2{}^+(A^2\Pi^a) + O({}^3P)$, so the translational energies of the fragments ($N + NO^+$) are larger than those of ($O + N_2{}^+$). But for H^- impact in DL process, the inner shell electron has a bigger opportunity to be ionized or excited due to the smaller impact parameter, and the parent ion N_2O^+ may populate higher $1\,{}^4\Pi$ excited states, and the main dissociation pathway for $N_2O^+(1\,{}^4\Pi)$ is $N_2O^+(1\,{}^4\Pi) \rightarrow N_2{}^+(X\ {}^2\Sigma_g{}^+) + O({}^3P)$. Thus, the fragments ($O + N_2{}^+$) have more translational energy. And for C^- and O^- impact, the bigger transferred energy makes the parent ion N_2O^+ populate on its highly excited state $C\ {}^2\Sigma^+$ or $1\ {}^4\Sigma^-$, and the dissociation fragment ions are $NO^+(X\ {}^1\Sigma^+) + N({}^4S)$ and $N_2{}^+(X\ {}^2\Sigma_g{}^+) + O({}^3P)$. Because the excited state of $N_2{}^+(X\ {}^2\Sigma_g{}^+) + O({}^3P)$ is larger than that of $NO^+(X\ {}^1\Sigma^+) + N({}^4S), (N + NO^+)$ may have more translational energy.

TABLE IV. The total translational energies of the fragments ($N + NO^+$) and ($O + N_2{}^+$) under H^-, C^-, and O^- impact in 15–30-keV energy region.

	H^- (SL)		H^- (DL)	
	$N + NO^+$ (eV)	$O + N_2{}^+$ (eV)	$N + NO^+$ (eV)	$O + N_2{}^+$ (eV)
15 keV	1.45	1.05	1.70	1.81
20 keV	1.35	1.26	1.60	1.98
25 keV	1.38	1.16	1.61	1.96
30 keV	1.25	1.21	1.50	2.01
	C^- (SL)		C^- (DL)	
	$N + NO^+$ (eV)	$O + N_2{}^+$ (eV)	$N + NO^+$ (eV)	$O + N_2{}^+$ (eV)
15 keV	4.15	2.80	6.11	4.16
20 keV	3.39	2.85	5.08	4.05
25 keV	3.50	2.77	5.16	3.89
30 keV	3.48	2.74	5.23	4.31
	O^- (SL)		O^- (DL)	
	$N + NO^+$ (eV)	$O + N_2{}^+$ (eV)	$N + NO^+$ (eV)	$O + N_2{}^+$ (eV)
15 keV	5.05	2.43	5.79	2.71
20 keV	4.38	2.81	5.84	3.60
25 keV	4.39	2.57	6.77	3.69
30 keV	4.01	2.94	5.92	4.87

IV. CONCLUSION

The relative dissociation fractions of N_2O ($N^+, O^+, N_2{}^+, NO^+$) are obtained under H^-,C^-, and O^- negative ions' impact in the incident energy from 15 to 30 keV. And with the impact energy increasing, more and more atomic ions are produced, and the fractions of molecular ions become smaller. That means the target molecules fragment more violently with bigger incident energy. And the fractions in the DL process

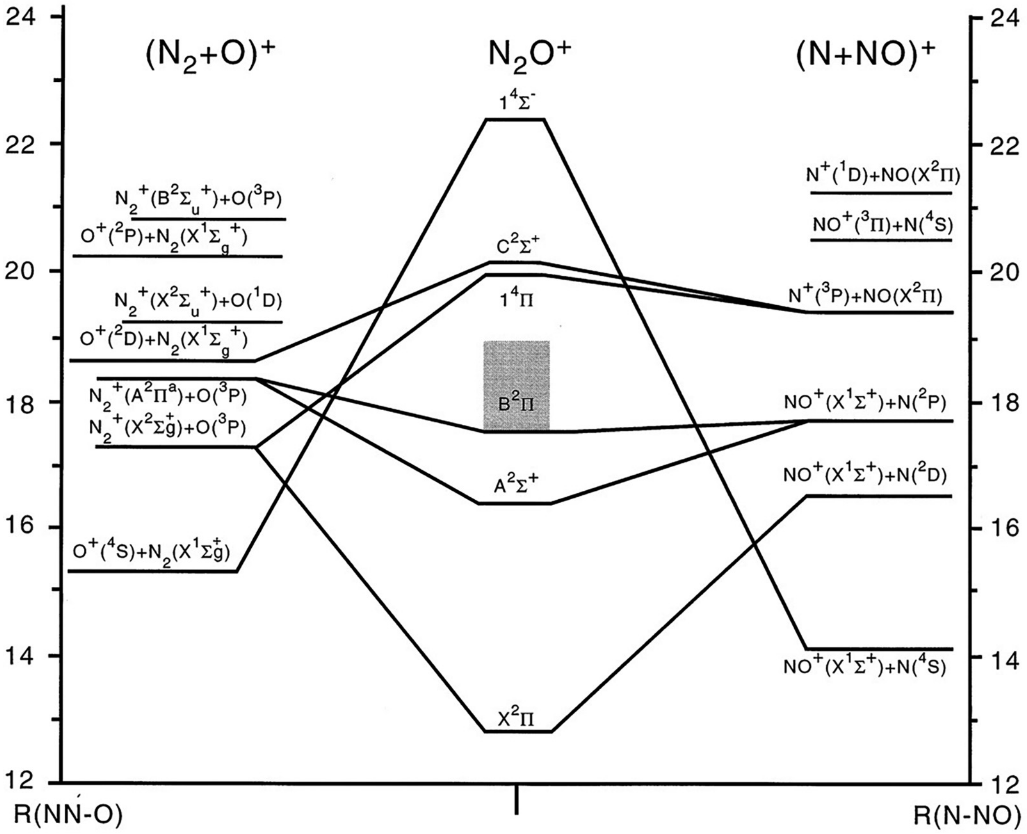

FIG. 8. Adiabatic correlation diagram for N_2O^+ following Richard-Viard [23] (we have changed $C\ ^2\Sigma^-$ to $C\ ^2\Sigma^+$).

are larger than those in the SL process for certain energies, especially in C^- and O^- impact. We also find that the fractions become greater with the projectile momentum increasing. In addition, we give the ratios of $O^+ + N_2^+/N^+ + NO^+$, and compare those with the earlier reported experimental results. And we interpret the major dissociation pathways of N_2O^{2+} in 15- to 30-keV H^-,C^-, and O^- impact by analyzing the peak slopes of different ion pairs in the coincidence spectra of two fragment ions. Finally, we obtain the translational energy of $(N + NO^+)$ and $(O + N_2^+)$ in the dissociation of N_2O^+.

ACKNOWLEDGMENTS

This work was supported by the Chinese National Science Foundation (Grant No. 11374062) and Shanghai Leading Academic Discipline Project No. B107.

---

[1] M. Alagia, P. Candori, S. Falcinelli, M. Lavollée, F. Pirani, R. Richter, S. Stranges, and F. Vecchiocattivi, Double photoionization of N_2O molecules in the 28–40 eV energy range. Chem. Phys. Lett. **432**, 398 (2006).

[2] B. P. Forster in *Climate Change 2007: The Physical Science Basis*, Contribution of Working Group I to the Fourth Assessment Report of the Intergovernmental Panel on Climate, 2007, edited by S. Solomon *et al.* (Cambridge University Press, New York, 2007), pp. 1–21.

[3] http://www.noaanews.noaa.gov/stories2009/20090827_ozone.html

[4] P. Bhatt, R. Singh, N. Yadav, and R. Shanker, Momentum spectroscopy of fragment ions of a multiply charged N_2O molecule under impact of 10-keV electrons, Phys. Rev. A **86**, 052708 (2012).

[5] S. D. Price, J. H. D. Eland, P. G. Fournier, J. Fournier, and P. Millie, Electronic states and decay mechanisms of the N_2O^{2+} dication, J. Chem. Phys. **88**, 1511 (1988).

[6] N. Levasseur and P. Millié, Potential energy surfaces of the low-lying states of N_2O^{++} and photo dissociation mechanisms, J. Chem. Phys, **92**, 2974 (1990).

[7] J. H. D. Eland and V. J. Murphy, Charge-separation reactions of N_2O cations formed by low- and high-energy ionization, Rapid Commun. Mass Spectrom. **5**, 221 (1991).

[8] L. J. Frasinski, P. A. Hatherly, and C. Codling, Multiphoton multiple ionisation of N_2O probed by three-dimensional covariance mapping, Phys. Lett. **A**, **156**, 227 (1991).

[9] T. LeBrun, M. Lavollee, M. Simon, and P. Morin, Dissociation dynamics of core excited N_2O, J. Chem. Phys. **98**, 2534 (1993).

[10] S. Hsieh and J. H. D. Eland, Reaction dynamics of three-body dissociations in triatomic molecules from single-photon double ionization studied by a time- and position-sensitive coincidence method, J. Phys. B **30**, 4515 (1997).

[11] A. Hishikawa, A. Iwamae, K. Hoshina, M. Kono, and K. Yamanouchi, Coulomb explosion dynamics of N_2O in intense laser-field: Identification of new two-body and

three-body fragmentation pathways, Res. Chem. Intermed. **24**, 765 (1998).

[12] M. Kübel *et al.*, Strong-field control of the dissociative ionization of N_2O with near-single-cycle pulses, New J. Phys. **16**, 065017 (2014).

[13] R. Karimi, É. Bisson, B. Wales, S. Beaulieu, M. Giguère, Z. Long, W.-K. Liu, and J.-C. Kieffer, N_2O ionization and dissociation dynamics in intense femtosecond laser radiation, probed by systematic pulse length variation from 7 to 500 fs, J. Chem. Phys. **138**, 204311 (2013).

[14] X. Zhou, P. Ranitovic, C. W. Hogle, J. H. D. Eland, H. C. Kapteyn, and M. M. Murnane, Probing and controlling non-Born–Oppenheimer dynamics in highly excited molecular ions, Nat. Phys. **8**, 232 (2012).

[15] Natalie A. Love and D. Stephen, Price Electron ionization of N_2O, Phys. Chem. Chem. Phys. **6**, 4558 (2004).

[16] J. Lopez, V. Tarnovsky, M. Gutkin, and K. Becker, Electron-impact ionization of NO, NO_2, and N_2O, Int. J. Mass Spectrom. **225**, 25 (2003).

[17] B. G. Lindsay, R. Rejoub, and R. F. Stebbings, Absolute cross sections for electron-impact ionization of N_2O, H_2S, and CS_2 from threshold to 1000 eV, J. Chem. Phys. **118**, 5894 (2003).

[18] P. Bhatt, R. Singh, N. Yadav, and R. Shanker, Relative partial ionization cross sections of N_2O under 10–25-keV electron impact, Phys. Rev. A **85**, 034702 (2012).

[19] Z. Zhao, J. Li, and X. Zhang, Experimental study of ionization of Ar by impact of anions, Nucl. Instrum. Methods Phys. Res., Sect. B **283**, 35 (2012).

[20] J. Li, Z. Zhao, and X. Zhang, Ionization and dissociation fractions of CO_2 under 10–30-keV H^-, C^-, and O^- negative-ion impact, Phys. Rev. A **86**, 052703 (2012).

[21] Z. Zhao, J. Li, and X. Zhang, Relative dissociation fractions of SF_6 under impact of 15-keV to 30-keV H^- and C^- negative ions, Phys. Rev. A **88**, 042708 (2013).

[22] D. Wang, Y. Fan, Z. Zhao, G. Min, and X. Zhang, Relative dissociation fractions of CF4 under 15–30 keV H^-, C^- and O^- negative ion impact, J. Phys. B: At. Mol. Opt. Phys. **49**, 165201 (2016).

[23] E. Kinmond, J. H. D. Eland, and L. Karlsson, Dissociation of N_2O^+ ions from the valence states reached byone-photon photoionisation, Int. J. Mass Spectrom. **185/186/187**, 437 (1999).

[24] M. Lange, O. Pfaff, U. Muller, and R. Brenn, Projectile fragment–ion fragment–ion coincidences (PFIFICO) following fast ion impact on SF_6, Chem. Phys. **230**, 117 (1998).

[25] M. Ueyama, H. Hasegawa, A. Hishikawa, and K. Yamanouchi, Concerted and sequential Coulomb explosion processes of N_2O in intense laser fields by coincidence momentum imaging, J. Chem. Phys. **123**, 154305 (2005).

[26] B. Siegmann, U. Werner, H. O. Lutz, and R. Mann, Two-particle Coulomb-fragmentation of N_2O in collisions with 5.9 MeV/u Xe^{43+} ions, http://citeseerx.ist.psu.edu/viewdoc/summary?doi=10.1.1.183.4006.

[27] Z. F. Sun, Z. Gao, X. K. Wu, G. Q. Tang, X. G. Zhou, and S. L. Liu, Excitation Spectra and Photodissociation Dynamics of the $B\ ^2\Pi$ State of the N_2O^+ Ion, Acta. Phys. -Chim. Sin. **31**, 829 (2015).

[28] X. Tang, M. Niu, X. Zhou, S. Liu, F. Liu, X. Shan, and L. Sheng, NO^+ formation pathways in dissociation of N_2O^+ ions at the $C\ ^2\Sigma^+$ state revealed from threshold photoelectron–photoion coincidencevelocity imaging, J. Chem. Phys. **134**, 054312 (2011).

[29] X. Tang, X. Zhou, B. Qiua, S. Liu, F. Liu, X. Shan, and L. Sheng, New insight into dissociative photoionization of N_2O at ∼20 eV usingthreshold photoelectron–photoion coincidence velocity imaging, J. Electron Spectrosc. Relat. Phenom. **196**, 43 (2014).